DOCK11 deficiency in patients with X-linked actinopathy and autoimmunity

Charlotte Boussard, Laure Delage, Tania Gajardo, Alexandre Kauskot, Maxime Batignes, Nicolas Goudin, Marie-Claude Stolzenberg, Camille Brunaud, Patricia Panikulam, Quentin Riller, et al.

Title: DOCK11 deficiency in patients with X-linked actinopathy and autoimmunity

Authors:
Charlotte Boussard,[1,*] Laure Delage,[1,*] Tania Gajardo,[2,†] Alexandre Kauskot,[3,†] Maxime Batignes,[4,†] Nicolas Goudin,[5] Marie-Claude Stolzenberg,[1] Camille Brunaud,[1] Patricia Panikulam,[2] Quentin Riller,[1] Maryse Moya-Nilges,[6] Jean Solarz,[3] Christelle Repérant,[3] Béatrice Durel,[7] Jean-Claude Bordet,[8] Olivier Pellé,[1,9] Corinne Lebreton,[10] Aude Magérus,[1] Vithura Pirabakaran,[1] Pablo Vargas,[11] Sébastien Dupichaud,[6] Marie Jeanpierre[1], Angélique Vinit,[12] Mohammed Zarhrate,[13] Cécile Masson,[14] Nathalie Aladjidi,[15, 16] Peter D. Arkwright,[17] Brigitte Bader-Meunier,[1, 18] Sandrine Baron Joly,[19] Joy Benadiba,[20] Elise Bernard,[21] Dominique Berrebi,[22] Christine Bodemer,[23] Martin Castelle,[18] Fabienne Charbit-Henrion,[10,24,25] Marwa Chbihi,[18] Agathe Debray,[26] Philippe Drabent,[27] Sylvie Fraitag,[27] Miguel Hié,[28],Judith Landmann-Parker,[29] Ludovic Lhermitte,[30] Despina Moshous,[18, 31, 32] Pierre Rohrlich,[20] Frank Ruemmele,[24] Anne Welfringer-Morin,[23] Maud Tusseau,[33] Alexandre Belot,[33,34,35] Nadine Cerf-Bensussan,[10] Marie Roelens,[36,37] Capucine Picard,[32,37,38] Bénédicte Neven,[1, 18] Alain Fischer,[38, 39, 40] Isabelle Callebaut,[41] Mickaël Ménager,[4,42, ‡] Fernando E. Sepulveda,[2,‡] Frédéric Adam,[3,‡] Frédéric Rieux-Laucat,[1,‡].

* Dr. Charlotte Boussard and Dr. Laure Delage contributed equally to this work.
† Dr. Gajardo, Dr. Kauskot, and Dr. Batignes contributed equally to this work.
‡ Dr. Ménager, Dr. Sepulveda, Dr. Adam, and Dr. Rieux-Laucat share senior authorship.

Affiliations:
[1]Université Paris Cité, Institut Imagine, Laboratory of Immunogenetics of Pediatric Autoimmune Diseases, INSERM UMR 1163; F-75015 Paris, France.

[2]Université Paris Cité, Institut Imagine, Laboratory of Molecular Basis of Altered Immune Homeostasis, INSERM UMR 1163; F-75015 Paris, France.

[3]INSERM, UMR_S1176, Université Paris-Saclay, F- 94276 Le Kremlin-Bicêtre, France.

[4]Université Paris Cité, Institut Imagine, Laboratory of Inflammatory Responses and Transcriptomic Networks in Diseases, Atip-Avenir Team, INSERM UMR 1163; F-75015 Paris, France.

[5]Necker Bio-image Analysis Platform, Structure Fédérative de Recherche Necker, INSERM US24, CNRS UMS3633, F-75015 Paris, France.

[6]Institut Pasteur, UTechS Ultrastructural BioImaging UBI, F-75015 Paris, France.
x
[7]Cell Imaging Platform, Structure Fédérative de Recherche Necker, INSERM US24, CNRS UMS3633, F-75015 Paris, France.

[8]Laboratoire d'Hémostase, Centre de Biologie Est, Hospices Civils de Lyon, F-68500 Bron, France.

[9]Flow Cytometry Core Facility, Structure Fédérative de Recherche Necker INSERM US24, CNRS UMS3633, F-75015 Paris, France.

[10]Université Paris Cité, Imagine Institute, Laboratory of Intestinal Immunity, INSERM UMR 1163; F-75015 Paris, France.

[11]Institut Necker Enfants Malades (INEM), INSERM U1151/CNRS UMR 8253, Université de Paris, 156-160 rue de Vaugirard, 75015 Paris, France.

[12]Sorbonne Université, UMS037, PASS, Plateforme de cytométrie de la Pitié-Salpêtrière CyPS; F-75013 Paris, France.

[13]Genomics Core Facility, Institut Imagine-Structure Fédérative de Recherche Necker, INSERM U1163 et INSERM US24/CNRS UAR3633, Université Paris Cite ; F-75015 Paris, France.

[14]Bioinformatics Core Facility, Institut Imagine-Structure Fédérative de Recherche Necker, INSERM U1163 et INSERM US24/CNRS UAR3633, Paris Cite University, Paris, France

[15]Centre de Référence National des Cytopénies Auto-immunes de l'Enfant (CEREVANCE), Bordeaux, France.

[16]Pediatric Oncology Hematology Unit, University Hospital, Plurithématique CIC (CICP), Centre d'Investigation Clinique (CIC) 1401, INSERM, Bordeaux, France.

[17]Lydia Becker Institute of Immunology and Inflammation, University of Manchester & Department of Pediatric Allergy and Immunology, Royal Manchester Children's Hospital, Oxford Road, Manchester, UK.

[18]Pediatric Immunology, Hematology and Rheumatology Department, Hôpital Necker-Enfants Malades, Assistance Publique-Hôpitaux de Paris (AP-HP); F-75015 Paris, France.

[19]Department of Pediatrics, Nîmes University Hospital, Nîmes, France.

[20]Department of Pediatric Hematology-Oncology, Nice University Hospital, Nice, France.

[21]Departement of General Pediatrics, Centre hospitalier de Mayotte, Mamoudzou, Mayotte, France.

[22]Department of Pediatric Pathology, Hôpital Robert-Debré, Hôpital Universitaire Robert-Debré, Assistance Publique-Hôpitaux de Paris, Paris, France.

[23]Department of Dermatology, referral Center for Genodermatoses (MAGEC), Assistance Publique-Hopitaux de Paris, Hôpital Necker–Enfants Malades, F-75015, Paris, France.

[24]Department of Pediatric Gastroenterology, Assistance Publique-Hopitaux de Paris, Hôpital Necker–Enfants Malades, F-75015, Paris, France.

[25]Department of Genomic Medecine for Rare Diseases, Assistance Publique-Hopitaux de Paris, Hopital Necker–Enfants Malades, F-75015, Paris, France.

[26]Departement of General Pediatrics and Infectious Diseases, Hôpital Trousseau, Assistance Publique-Hôpitaux de Paris, Paris, France.

[27]Department of Anatomopathology, Assistance Publique-Hopitaux de Paris, Hôpital Necker–Enfants Malades, F-75015, Paris, France.

[28]Sorbonne Université, Assistance Publique - Hôpitaux de Paris, Groupement Hospitalier Pitié-Salpêtrière, Service de Médecine Interne 2, Institut E3M, Inserm UMRS 1135, Centre d'Immunologie et des Maladies Infectieuses (CIMI-Paris), Paris, France.

[29]Sorbonne Université, Pediatric Hematology Oncology department, Hôpital Armand-Trousseau, AP-HP, F-75012-Paris, France.

[30]Laboratory of Onco-Haematology, AP-HP, Université de Paris Cité, Institut Necker-Enfants Malades, INSERM UMR 1151, F-75015, Paris, France

[31]Université Paris Cité, Imagine Institute, Laboratory of Genome Dynamics in the Immune System, INSERM UMR 1163, F-75015 Paris, France.

[32]French National Reference Center for Primary Immune Deficiencies (CEREDIH), Necker-Enfants Malades University Hospital, AP-HP; F-75015 Paris, France.

[33]The International Center of Research in Infectiology, Lyon University, INSERM U1111, CNRS UMR 5308, ENS, UCBL, Lyon, France.

[34]National Referee Centre for Rheumatic and Autoimmune Diseases in Children, RAISE, Paris and Lyon, France.

[35]Pediatric Nephrology, Rheumatology, Dermatology Department, Hôpital Femme Mère Enfant, Hospices Civils de Lyon, 59 Bd Pinel, 68677, Bron Cedex, France.

[36]Université Paris Cité, Paris, France.

[37]Study Center for Primary Immunodeficiencies (CEDI), Hôpital Necker-Enfants Malades University, AP-HP; F-75015 Paris, France.

[38]Université Paris Cité, Imagine Institute, INSERM UMR 1163; F-75015 Paris, France

[39]Department of Pediatric Immuno-Haematology and Rheumatology, Reference Center for Rheumatic, AutoImmune and Systemic Diseases in Children (RAISE), Hôpital Necker-Enfants Malades, Assistance Publique – Hôpitaux de Paris (AP-HP); F-75015 Paris, France.

[40]Collège de France ; F-75231 Paris, France.

[41]Sorbonne Université, Muséum National d'Histoire Naturelle, CNRS UMR 7590, Institut de Minéralogie, de Physique des Matériaux et de Cosmochimie, F-75005 Paris, France.

[42]Labtech Single-Cell@Imagine, Imagine Institute, INSERM UMR 1163; F-75015 Paris, France.

Corresponding author:
Dr Frédéric Rieux-Laucat, Institut *Imagine*, 24 Boulevard du Montparnasse, 75015, Paris, France ; Email: frederic.rieux-laucat@inserm.fr.

ABSTRACT

Dedicator of cytokinesis (DOCK) proteins play a central role in actin cytoskeleton regulation. This is highlighted by the DOCK2 and DOCK8 deficiencies leading to actinopathies and immune deficiencies. DOCK8 and DOCK11 activate CDC42, a RHO-GTPase involved in actin cytoskeleton dynamics, among many cellular functions. The role of DOCK11 in human immune disease has been long suspected but has never been described so far. We studied eight male patients, from seven unrelated families, with hemizygous *DOCK11* missense variants leading to reduced DOCK11 expression. The patients were presenting with early-onset autoimmunity, including cytopenia, systemic lupus erythematosus, skin, and digestive manifestations. Patients' platelets exhibited abnormal ultrastructural morphology and spreading as well as impaired CDC42 activity. *In* vitro activated T cells and B lymphoblastoid cell lines (B-LCL) of patients exhibited aberrant protrusions and abnormal migration speed in confined channels concomitant with altered actin polymerization during migration. A DOCK11 knock-down recapitulated these abnormal cellular phenotypes in monocytes-derived dendritic cells (MDDC) and primary activated T cells from healthy controls. Lastly, in line with the patients' autoimmune manifestations, we also observed abnormal regulatory T cells (Tregs) phenotype with profoundly reduced FOXP3 and IKZF2 expression. Moreover, we found a reduced T cell proliferation and an impaired STAT5B phosphorylation upon IL2 stimulation of the patients' lymphocytes. In conclusion, DOCK11 deficiency is a new X-linked immune-related actinopathy leading to impaired CDC42 activity and STAT5 activation, and associated with abnormal actin cytoskeleton remodeling as well as Tregs phenotype culminating in immune dysregulation and severe early-onset autoimmunity.

Running title: DOCK11 actinopathy associated with autoimmunity

Key points:

- DOCK11 deficiency is a new X-linked immune-related actinopathy.
- DOCK11 deficiency leads to impaired CDC42 activity, abnormal actin cytoskeleton remodeling, and immune dysregulation.

Word count: 4096, Abstract word count: 245, Figures/Tables: 6/1, Number of references: 45.

Introduction

Immune-related actinopathies are inborn errors of immunity (IEIs) due to gene defects impacting actin cytoskeleton remodeling. More than 20 entities are described so far[1].Actin cytoskeleton remodeling is a dynamic and tightly regulated process crucial for cell shape modifications, cell adhesion, motility, and other main cellular functions[2]. Rho-GTPases, RAS-related GTP-binding proteins, such as RAC, CDC42, and RHO, are key players in the intracellular actin reorganization[3,4]. The phenotypic spectrum of *RAC2* mutations ranges from granulocytes deficiency (loss-of-function mutations) to SCID with bone-marrow hypoplasia (gain-of-function mutations)[5]. *De novo* mutations in *CDC42* were recently found in patients

presenting with Takenouchi-Kosaki syndrome, associating features such as macrothrombocytopenia and developmental abnormalities, or with neo-natal cytopenia with dyshematopoiesis, autoinflammation, rash and hemophagocytic lymphohistiocytosis (HLH), termed NORCAH syndrome[6] . Rho-GTPases are activated by Guanine Exchange Factors (GEFs), such as dedicator of cytokinesis (DOCK) family members like DOCK2 and DOCK8[7]. Biallelic mutations in *DOCK2* result in early-onset invasive bacterial and severe viral infections and T cell lymphopenia[8]. *DOCK8* mutations also result in severe bacterial, viral, and fungal infections, as well as eczema and severe environmental allergies[9]. These descriptions highlight the predominant role of DOCK protein members in immune-related actinopathies[10]. A role of DOCK11 in human immune disease has been long suspected but never described so far. Here we identified seven hemizygous mutations in *DOCK11*, a member of the DOCK-D subfamily, in eight patients with early-onset autoimmunity, including autoimmune cytopenia and systemic lupus erythematosus (SLE).

Methods

This section briefly describes the methods; further details are provided in the supplemental Appendix. Before the study, all patients signed informed consents approved by the CERAPH-Centre (IRB: #00011928). The biological samples are part of Inserm UMR1163/Imagine collection declared to the French Ministère de la recherche (CODECOH n° DC-2020-3994).

Protein structure analysis

3D structure prediction of DOCK11 protein was performed by combining information from literature-described structures and AlphaFold2 predictions[11]. The detailed method is described in the supplemental appendix.

Genetic and functional analysis

Whole exome (WES) and Sanger sequencing, mass cytometry, ELISA and G-LISA, confocal microscopy, migration assays, and *DOCK11* knock-down methods are detailed in the supplemental appendix.

Statistical analysis

Statistical analyses were performed using GraphPad Prism6 (GraphPad, La Jolla, CA, USA). Data were analyzed by one-way ANOVA followed by a post-hoc test, or unpaired non-parametric Mann-Whitney tests or Kruskal-Wallis' tests as indicated in the figure legends. Differences were considered significant when $p < 0.05$.

Data sharing statement

For original data, please contact frederic.rieux-laucat@inserm.fr.

Results

Clinical and biological features of the cohort

Eight male patients (7 to 29 years of age) from seven families of various ethnic origins were studied. Clinical and biological data are summarized in Table 1, Table S1, and Fig. S1. Detailed clinical cases are in the Supplemental appendix.

All patients presented early-onset autoimmunity at a median age of 5 years (range, 1 to 14 years). Five patients (A, C, E, F, G) had autoimmune cytopenia (Table 1). Twin patients (D1 and D2) had systemic lupus erythematosus (SLE). Patient B had a severe Rheumatoid Factor (RF) positive polyarticular juvenile arthritis and recurrent hemolytic anemia with positive Coombs tests. In addition, patient F had an auto-inflammatory syndrome with lymphoproliferation (Suppl. Appendix).

Five patients (A, C, D1, D2, F) presented with various cutaneous manifestations (detailed in Table1, Fig.1A, and S1), and four patients (A, B, D1, F) with digestive manifestations (Table 1 and Fig. S2). None of the patients presented with recurrent or severe infections, allergies nor bleeding disorders.

Among the maternal carriers, patient B's mother had metastatic melanoma and has been treated with immunotherapy; patient C's mother died of colorectal cancer at age 52.

Hemizygous deleterious mutations in *DOCK11*

Seven different hemizygous missense variants of *DOCK11* were identified by Whole-exome sequencing (WES) (Fig. 1B) in seven unrelated and non-consanguineous families. All six mothers tested carried the gene variants (Fig. S3A). We assessed the expression of the mutant and wild-type alleles in $CD4^+$, and $CD8^+$ T cells, B cells and monocytes in two mothers. The expression of both DOCK11 alleles was similar, indicating a global random X-inactivation in T and B cells as well as in monocytes (Fig S3B). These mutations were predicted to be deleterious *in silico,* and five are private variants (Fig. S3A). The mutated amino-acids are located in distinct domains of the DOCK11 protein (Fig 1B). Prediction of DOCK11 protein 3D structure allowed to apprehend mutations' potential deleterious impact (Fig. 1C-D and Fig. S4) and suggests that the variants may cause abnormal protein folding or directly impact DOCK11 interactions with its partners. Finally, DOCK11 expression was variably reduced in lysates from patients' activated T cells (Fig. 1E).

***DOCK11* mutations impair platelets functions and morphology**

Platelets play a central role in ITP and participate in the immune dysregulation in SLE pathogenesis[12]. As four patients presented with immune thrombocytopenia (ITP) and two patients with SLE, we investigated the impact of *DOCK11* mutations on platelet functions.

A significant decrease in the expression of DOCK11 was observed in the patients' platelets compared to healthy donors (Fig. 2A).

Patients' platelet counts were normal or subnormal, except for patients A and C, who presented mild to severe thrombocytopenia (Fig. 2B) but without glycosylation profile defect (Fig. S5A). Platelet size was also normal for the patients, except for patient A who exhibited macroplatelets (Fig. 2C and Fig.S5B). Moreover, electron microscopy ultrastructure analysis revealed abnormal morphology with elongated platelets in patients D1, D2, and G, contrasting with the discoid shape of resting platelets in healthy donors (HDs) (Fig. 2D-F).

Five, out of six patients tested, exhibited a defect of αIIbβ3 integrin activation at low concentrations of thrombin and convulxin (Fig. S5C), indicating a thrombopathy. Of note, the

expression of the main platelet receptors, glycoprotein (GP)Ibα, GPVI and αIIbβ3 integrin was normal in patients, except for patient A whose αIIbβ3 level was reduced (Fig. S5D). Analysis of platelet morphologies during platelet adhesion on various matrices (Fig. 2G and 2H and S5E) identified discoid platelets (resting stage), platelets with filopodia (intermediate morphological stage), and platelets with lamellipodia or full spreading (final morphological step)[13]. All patients exhibited an abnormal frequency of platelets at the final stage, except for patient D2, who exhibited more resting platelets. These results indicate that the patients' platelets exhibit abnormal morphological modifications during platelet adhesion and spreading. Of note, platelet functional assays were also performed for two mothers. A normal integrin αIIbβ3 activation was observed after stimulation of platelets by thrombin or convulxin and normal platelet morphologies distributions after adhesion (Figure S6A-B). Since DOCK11 is a GEF activating CDC42[14], CDC42 activation was evaluated by G-LISA in patients' platelets upon thrombin activation (Fig. 2I). In all tested patients (A, D1, D2, F, and G), platelets exhibited impaired CDC42 activity, providing a rationale for the lower frequency of filopodia stage upon adhesion and suggesting that *DOCK11* mutations are loss-of-function. Predominant lamellipodia or full spreading of patient platelet suggested an impact on others Rho-GTPases, such as RhoA[15]. In two patients tested (A and F), the RhoA activity was increased (Fig. S5F). This was mimicked by pharmacological treatment of healthy donors' platelets with Cdc42 inhibitor. In this condition, the RhoA activity was also increased (Fig. S5F). Taken together, these results indicate an imbalance in the CDC42/RHOA activity in the patients' cells.

DOCK11 mutated cells present abnormal morphological features

TCR-activated T cells from patients or HDs were spread on coverslips previously coated with poly-L-lysine (PLL), used as internal control, or with anti-CD28 and anti-CD3 antibodies at different concentrations (Fig. 3A). On the antibodies-coated coverslips, activated T cells tended to increase their spreading area along with the concentration of anti-CD3 antibody. At a mild concentration (0.1µg/mL), patients' T cells showed reduced circularity and increased area, probably as a consequence of higher numbers of protrusions formed by *DOCK11* mutated T cells (Fig. S7A). At a higher anti-CD3 concentration (1 µg/mL), mutated *DOCK11* T cells had a larger spreading area than the healthy donors (Fig. 3A). Notably, pharmacological activation of CDC42 restored cell spreading area to control levels (Fig. 3A). These results were confirmed in activated T cells from HDs after *DOCK11* sh-RNA inactivation (Fig. S7B).

Then, we analyzed morphologies of B-lymphoblastoid cell lines (B-LCL) after spreading on anti-CD44 coated coverslips (Fig. 3B). In these conditions, some B-LCL cells from patients exhibited an abnormal morphology, with numerous fine and long protrusions (Fig. 3B).

Finally, *DOCK11* sh-RNA inactivation was also performed in monocyte-derived dendritic cells (MDDC) from healthy donors. DOCK11 expression was reduced by almost 80% at the mRNA and protein levels (Fig. S7B). After activation and spreading, *DOCK11* inactivated MDDC had larger and more prominent protrusions (Fig. S8A-B) and produced more IL-1ß cytokine (Fig. S8C). Moreover, ruffles were aberrant and not comparable to the cells transfected with the scramble sh-RNA (Fig. 3C).

Finally, primary skin-derived fibroblasts from patient A revealed abnormal protrusions compared to healthy donor fibroblasts (Fig. S9).

Overall, our results suggest that DOCK11 deficiency impairs the morphology of several cell lineages.

DOCK11 mutations impact leukocytes migration and polarization of actin cytoskeleton under confinement.

To confirm that *DOCK11* variants impair actin cytoskeleton dynamics in lymphocytes, we next compared the spontaneous migratory capacity of activated T and B-LCL cells from HDs and DOCK11 patients (A to G) under confinement (Fig. 4A).

As previously described[16], human activated HD T cells presented constant trajectories with few directional changes (Fig. 4B). In contrast, all patients' derived T cells were faster than their HD counterpart (Fig. 4C). Of note, patient B's mother T cells had a speed migration similar to healthy donors (Figure S6C). Similarly, patient-derived B-LCL had higher migration speeds (Fig. S10A). To determine whether the increased speed of DOCK11-deficient cells correlated with alterations in actin polymerization, we assessed the front-rear distribution of actin in T cells fixed during migration in microchannels. In agreement with previous work[16], HD cells presented a bimodal actin-distribution, at the front and the rear of the cells (Fig. 4D). In contrast, DOCK11-deficient cells accumulated more actin at the rear of the cell (i.e., reduced front/rear actin ratio) in tested patients, consistent with the increased speed of these cells (Fig. 4C-D).

Mechanistically, the motility of activated T cells in microchannels depends on the balance in actin polymerization at the front (reflecting CDC42 activity) and rear (reflecting RHOA activity) of the cell[17]. These results were also observed in activated T cells from HDs after *DOCK11* sh-RNA inactivation (Fig. S10C).

Considering that DOCK11 has been associated with CDC42 activation [7,14], we hypothesized that the DOCK11 defects could reduce the activity of actin nucleators at the leading edge, which would displace the balance of actin polymerization and increase polymerization at the rear of the cells (thus increasing their speed). To test this hypothesis, HD T cells were treated with a pharmacological RAC1/CDC42 inhibitor. This treatment increased the speed of control T cells and impaired the front-rear ratio of actin polarization, recapitulating the alterations displayed by the DOCK11-deficient cells (Fig. 4E, figure S10D). Altogether our results suggest that DOCK11 is a critical regulator of the actin cytoskeleton dynamics and leukocytes migration under confinement.

DOCK11 deficiency results in abnormal Tregs phenotype and STAT5B activation in lymphocytes.

We next analyzed the impact of DOCK11 deficiency on the immune phenotype and some immune functions. Flow cytometry immunophenotyping revealed variable alterations of circulating immunoglobulins and B cell subsets, especially increased frequencies of $CD21_{low}$ and transitional B cells (Table 1 and Sup. Table1). Elevated concentrations of APRIL and BAFF were found in plasma patients (Fig. S11). Elevated plasma concentrations of inflammatory cytokines were also observed in most patients (Fig. S11). Mass cytometry immunophenotyping on whole blood did not reveal major alterations of cell subsets except for reduced proportions of early and late NK cells, mucosal-associated invariant T (MAIT) cells, and memory B cells

(Fig.5). Of note, CD57 expression was significantly increased in CD4+ T cells and γδ T cells (Fig. S12).

Autoimmune manifestations were prominent in all patients. In some cases, severe autoimmune enteropathy, reminiscent of the clinical presentation of FOXP3 deficient patients, suggested possible Tregs dysfunctions[18]. Tregs lymphocytes, were first analyzed using the $CD4^+CD25^+CD127_{low}$ surface markers. Despite a slight decrease in patient F, the proportion of this subset is comparable to the controls in the two other patients tested (Fig. 6A). Conversely, we observed a substantial reduction in the expression of FOXP3, and to a lesser extent, of HELIOS, by analyzing intracellular staining (Fig.6B). Therefore, the proportion of activated Tregs defined as CD4+ FOXP3+ HELIOS+, was lower in these patients compared to controls (Fig. 6B). These results suggested that DOCK11 could be involved in the regulation of FOXP3 in Tregs. Among multiple factors regulating the FOXP3 transcription, STAT5B activation has been described as a main regulator of FOXP3[19]. Consistent with the reduced FOXP3 expression in Tregs, we found a reduced activation of STAT5B in the patients' T cells compared to healthy donors upon IL2 stimulation (Fig. 5C-D). In contrast we observed a normal or slightly reduced IL6-dependent STAT3 activation in the patients' cells, suggesting a major impact of DOCK11 deficiency on the IL2-STAT5 pathway only (Fig S13C). A decreased IL2-induced STAT5B activation is also observed in B lymphocytes and MAIT cells (Fig. 5C-D). More importantly, we confirmed a decreased IL2-induced STAT5B activation in T cells from patients (Fig. S13A) and from healthy donors, in which we induced a decrease in DOCK11 expression by knock-down (Fig. S13B). Consistently, we also observed a variably reduced proliferation upon CD3 stimulation in activated T cells from five patients compared to HDs (Fig. S14). Overall, these results suggest that the DOCK11 deficiency is associated with an impairment of the IL2-STATB pathway in different patients' lymphocyte subsets as well as in DOCK11 knocked-down T cells from healthy donors.

Discussion:

We identified seven private and rare hemizygous missense mutations of *DOCK11* leading to early onset autoimmune disease. Human DOCK11 deficiency has never been described so far. DOCK11 is a GEF protein of the DOCK-D family. Mostly expressed in hematopoietic cells, DOCK11 is suspected to impact actin cytoskeleton remodeling through CDC42 activation, an important Rho-GTPase [8,16].

All *DOCK11* mutations are predicted to be deleterious, and 3D modeling suggests that they could impact the stability of the protein conformation or its interactions with putative partners. Accordingly, reduced DOCK11 expression was observed in patients' platelets and lymphocytes. The different variants, leading to a variable protein expression, may account for the variable clinical phenotypes observed in patients. Nevertheless, all tested patients showed reduced CDC42 activity in platelets, highlighting the abnormal function of the *DOCK11* mutants. Decreased CDC42 activity in platelets was associated with impaired platelet morphology, spreading, and activation. The spreading of platelets implicates Rho-GTPases such as CDC42, RAC, and RHO via integrins activation[13,15]. Some studies suggested that CDC42 is involved in platelet filopodia formation and spreading on fibrinogen[20]. RhoA activity, implicated in lamellipodia and stress fiber formation of platelets, was increased in the patients

tested and increased after inhibition of Cdc42 in healthy donors' platelets. Stimulated platelets from patients had a higher proportion of spread platelets, with deficient filopodia formation, reflecting a potentially disrupted balance between the Rho-GTPases Cdc42 and RhoA.

Of note, reduced integrin αIIbβ3 activation was observed in patients' platelets upon stimulation with an agonist at low concentration but not at high concentration. These results are consistent with a partial impairment of CDC42 activation in patients' platelets[21]. Interestingly, circulating anti-αIIbβ3 antibodies were detected in patient A, who developed severe ITP with highly fluctuating platelet counts. The absence of significant bleeding disorder in DOCK11 patients, with or without ITP, suggests that the hemostatic role of platelets is not impacted. Platelet extensive exploration highlighted impaired actin cytoskeleton, abnormal activation, and disrupted Rho-Gtpase balance in all patients tested, regardless of the presence or absence of thrombocytopenia. Functional non-hemostatic thrombopathy may impair the immunoregulation role of platelets as described in other autoimmune diseases[12,22,23].

T and B cell development and function can be disrupted in immune-related actinopathy, as previously described in other DOCK deficiencies[24,26]. Patients' T cells and *DOCK11* knock-down activated T cells from healthy controls exhibited aberrant cytoskeleton rearrangement with larger spreading areas and more protrusions, which could impair migration, sensing, or interactions with other immune cells[27,28]. Indeed, migration speed under confinement was increased concomitantly with an abnormal actin polymerization at the rear during migration of the patients' activated T cells and DOCK11 knock-down model, a finding consistent with an impaired balance in the activity of Rho-GTPases[29]. Moreover, the pharmacological inhibition of RAC/CDC42 in healthy donor-derived T cells reproduced the aberrant spreading, faster migration, and impaired actin polarization, as observed in patients-derived T cells. Conversely, incubating the patients' T cells with a CDC42 activator restored normal spreading. Taken together, these results support the conclusion that DOCK11 deficiency impairs the balance between CDC42 and RhoA activity in activated T cells, as observed in platelets. Interestingly, a faster migration was also observed in patients B-LCL, indicating that DOCK11 would be a general regulator of lymphocyte migration. Lastly, we observed aberrant protrusions and ruffles upon reduced protein expression by the *DOCK11* knock-down in MDDC from healthy donors. This is reminiscent of the role of mouse Dock11 (Zizimin2) in the actin remodeling of bone marrow-derived dendritic cells[30]. The abnormal cell shape of DOCK11 inactivated MDDC, and their increased production of IL-1β suggest that the patients' dendritic could contribute to the immune dysregulation observed in patients.

The patients' immunological phenotyping showed an abnormal distribution of the B cell subsets with increased circulating BAFF and APRIL in the patients' plasma. Impaired balance of B cell populations in favor of transitional and $CD21_{low}$ B cells with elevated cytokine levels of the BAFF complex may promote autoimmunity in patients, as already described in other immune disorders[31] . The Dock11 deficient mouse model (known as the Zizimin 2 knock-out, the mouse counterpart of DOCK11) showed disturbed B cell subsets distribution[32]. But surprisingly, these mice did not develop autoimmune manifestations. However, many examples of genetic defects lead to very different phenotypes in humans and mice. For example, Lrba knock-out in mice has no impact on regulating the immune response, whereas LRBA-deficient patients present with Primary immune deficiency and a broad spectrum of autoimmune manifestations[33,34].

T cell subsets' distribution was not overtly disturbed except for a reduced proportion of MAIT cells. NK cell subsets were also low in patients but without obvious clinical consequences such as viral infections or macrophage activation syndrome. Immunosenescence of T cells was increased in patients, consistent with the immune-aging role of DOCK11 suggested by the mouse models [30,32]. Increased pro-inflammatory Th1 and Th17 cytokines in the patients' plasma, without any documented infection, suggest a possible immune dysregulation that could be the cause or the consequence of the patients' autoimmune and auto-inflammatory phenotypes.

All patients presented with various clinical phenotypes, including severe autoimmune cytopenia, SLE, auto-inflammatory syndrome, or lymphoproliferation. Most patients had inflammatory bowel disease (IBD), and some had various immune-related skin manifestations. Importantly, none of the patients had severe or recurrent infections, and vaccinal responses were normal in the two tested patients indicating an overall normal humoral response.

The severe early-onset autoimmune enteropathy observed in some patients was reminiscent of the prominent symptoms observed in FOXP3 deficient patients, suggesting a potential Tregs defect in the DOCK11 patients[18]. Whereas we observed a mildly reduced proportion of Tregs in one patient, we found the expected proportion of this subset in the other patients. However more strikingly, we found a markedly decreased expression of FOXP3, the master Tregs transcription factor, and HELIOS to a lesser extent. These two transcription factors are essential to sustain the Tregs suppressive functions[35,36]. Moreover, Tregs are highly dependent of IL2 and its downstream signaling pathway, as observed in IL2, IL2R, and STAT5B deficiencies[37,38], all characterized by impaired Tregs function and overt autoimmune manifestations. Interestingly, we observed a reduced STAT5B activation in the patients' T and B cells upon IL2 stimulation. This was corroborated by a slight but consistent reduction in T cell proliferation. More importantly, the reduced IL2-induced STAT5B activation is observed in DOCK11 knock-down T cells from healthy controls. All these results point to a global IL2-STAT5 signaling impairment in the context of DOCK11 deficiency and provide a molecular basis for the underlying mechanisms leading to autoimmunity in the patients.

One challenging observation is that DOCK11 patients develop overt autoimmune manifestations but not viral, bacterial, or fungal infections, whereas DOCK8 patients predominantly suffer from recurrent sinopulmonary and mucocutaneous infections, severe allergy with elevated serum levels of IgE but mild or any autoimmune symptoms[39]. Nevertheless, both defects are leading to a reduced CDC42 activity[40], which therefore seems to be the main cause of the loss of cell shape integrity and abnormal motility, and indicates that both GEFs are non-redundant and possibly working in concert in this process. This also indicates that the impaired CDC42 activation is not fully involved in the pathophysiological mechanisms of each defect. The list of DOCK partners is probably far from being wholly defined. Since DOCK8 and DOCK11 belong to different DOCK subfamilies, one can anticipate that they may share common but also different partners. In addition, their respective expression may differ according to immune cell subsets. In humans, it was reported that the DOCK8 deficiency is associated with a reduced STAT3 activation in various lymphocyte subsets, consistent with the observation that DOCK8 deficient patients share common clinical and biological features with STAT3 deficient ones such as hyper IgE, food allergy, and mucocutaneous infections related to impaired Th17 function[41]. In this study, we uncovered an

IL2-STAT5 (but not an IL6-STAT3) signalization defect and an abnormal Tregs phenotype, two findings consistent with the development of autoimmunity. Surprisingly a similar Tregs dysfunction has also been described in DOCK8 deficient patients, despite the lack of prominent autoimmunity, further blurring the understanding of the mechanisms involved[42]. Very interestingly, whereas Dock8 deficient mice have impaired Tregs function but do not develop autoimmunity, Treg-specific Dock8 deficient mice have lymphoproliferation, autoantibodies production, and enteropathy [43], thus suggesting that DOCK8 deficiency in conventional T cells, or maybe in other immune subsets, is protecting from the onset of autoimmunity in patients.
On the other hand, one might speculate that the impairment of some immune subsets, such as the MAIT cells, for instance, or that the platelets abnormalities observed in the DOCK11 deficient patients could contribute to the development of autoimmunity. Lastly, the DOCK11 expression pattern is not restricted to the hematopoietic compartment but also allows its expression in various skin and intestinal cells[44]. Accordingly, we observed aberrant protrusions of primary skin fibroblasts derived from patient A, suggesting an impact on the actin cytoskeleton remodeling in non-hematopoietic cells. Therefore, it is not excluded that the DOCK11 deficiency in non-hematopoietic cells contributes to tissue inflammation, possibly driving the autoimmune response to these tissues.
Another sharp contrast with the DOCK8 deficiency is the lack of overt viral infection despite the impact of the DOCK11 deficiency on T cell migration and possibly other immune cells, suggesting that DOCK11 deficient T cells could convey a normal tissue surveillance, possibly in line with a normal or only slightly reduced STAT3 activation. In addition to differential expression in immune cells, this might also relate to DOCK11-specific functions. Recently, Ide et al. identified DOCK11 as a potential therapeutic target to prevent persistent HBV infection[45]. In this work, the authors suggested that DOCK11 plays a role in the retrograde trafficking in the HBV infection and contributes to maintaining cccDNA. If this mechanism holds for other Herpes viruses, the DOCK11 deficiency might passively protect from those viral infections.

In conclusion, this study describes a new X-linked immune-related actinopathy in eight patients with severe early-onset autoimmunity, including SLE, caused by *DOCK11* hemizygous mutations. Platelets, T, and B cells from DOCK11 deficient patients showed aberrant cytoskeleton remodeling with impaired CDC42 activity. The regulation of Foxp3 in Tregs is impaired, involving the IL2-STAT5B pathway. Our results underscore the crucial DOCK11 function in hematopoietic cells and provide a novel example of the implication of actin cytoskeleton in human immune disorders. Further analyses are warranted to better understand the complex interactions between DOCK11 with other DOCK molecules, notably DOCK8, as well as to better characterize the molecular link with the IL2-STAT5B pathway. This can provide key information to help clinicians to adopt the best therapeutic options. All patients have been treated with different immunosuppressive drugs that variably controlled the autoimmune manifestations. Considering that the DOCK11 deficiency is impacting the cell shape, the mechanical migration or the adhesion of circulating cells, T regulators and possible tissue-resident immune cells, allogenic hematopoietic stem cell (HSCs) transplantation could be contemplated as a therapeutic option.

Limits of the study: all patients present with autoimmune features that may reflect biased recruitment in our laboratory. Furthermore, the identified mutations seem to confer a partial DOCK11 defect. Therefore, we do not exclude that *DOCK11* mutations could be associated with a broader or more severe clinical phenotype, including autoinflammatory diseases [40,41,42,] or combined immune deficiencies, notably in patients with a complete DOCK11 deficiency.

Acknowledgments, funding, and disclosures:

We sincerely thank the patients and their families for participating in the study.
We thank Noémie Paillon and Dr Juan-Jose Saez-Pons from the laboratory of Dr Claire Hivroz at Institute Curie, Université PSL, U932 INSERM, Integrative Analysis of T cell Activation Team, Paris, France for the help with T cell spreading assay. We thank the CIQLE Centre d'Imagerie Quantitative Lyon-Est (France) for expert technical assistance with the electron microscopy studies. We thank Dr Dominique Lasne and Pr Delphine Borgel at Necker Children's Hospital (Hematology Department, Paris) for their assistance with platelet studies.
We thank the staff from the *Imagine* genomic, bioinformatics and cytometry core facility and the Salpétrière CyPS cytometry facility for advice and technical assistance. Lastly, we thank the attending physicians for their support and for coordinating the patients' clinical care and sample collection.
The study was funded by the Institut National de la Santé et de la Recherche Médicale (INSERM), the French government (managed by French National Research Agency (Agence Nationale de la Recherche) through the "Investissements d'avenir" program (Institut Hospitalo-Universitaire Imagine, grant reference: ANR-10-IAHU-01; Recherche Hospitalo-Universitaire, grant reference: ANR-18-RHUS-0010)), and other grants from the Agence National de la Recherche (ANR-18-CE17-0001 "Action", ANR-18-CE15-0017), the Fondation pour la Recherche Médicale (grant reference: Equipe FRM EQU202103012670). The authors acknowledge the Centre de Référence Déficits Immunitaires Héréditaires (CEREDIH), and the Centre de Référence des cytopénies auto-immunes de l'enfant (CEREVANCE) which allowed patients enrolment trough the OBS'CEREVANCE and ACTION cohorts.
This work was also supported by several grants. C.B. was a recipient of an INSERM "poste d'accueil" program and was awarded the Société Française de Pédiatrie prize. L.D. received a grant from the Imagine Thesis Award program. Q.R. received an Institut Imagine MD-PhD fellowship (funded by the Fondation Bettencourt Schueller) and a Société Nationale Française de Médecine Interne (SNFMI) fellowship.
The graphical abstract was created with BioRender.com.

Authorship contributions

Conceptualization, C.B., L.D., T.G., A.F., A.K., F.A., F.E.S., I.C, F.R-L.; Methodology, I.C., P.V.; Investigation, C.B., LD., T.G., A.K., M.B., C.Bru., B.D, M.M.-N., J.S., C.R., J-C.B., P.P., M-C.S., O.P., A.M., V.P., P.V., S.B., A.V., M.Z., C.M., M.R.; Data Curation, L.D, N.G., I.C., Q.R. C.M.; Formal Analysis, C.B., L.D., I.C., T.G., P.P., Q.R.; Writing – Original Draft, C.B.,

L.D., T.G, F.E.S., I.C., A.K, F.A., F.R-L.; Writing, Review & Editing, I.C., Q.R., N.A., P.D.A., M.C., P.P., N.C-B., F.C-H., S.F., P.D., L.L., D.M., P.R., A.W-M., M.R., B.N., J-C.B., A.M., A.K., F.A., M.B., M-C.S., C.B., L.D., F.R-L.; Visualization, I.C., L.D., C.B., Q.R., N.G., T.G., P.P., F.A., A.K., M.M-N, B.D., J-C.B., T.G.; Resources, C.L., N.A., P.D.A., B.B-M., S.B-J., A.B., J.B., E.B., D.B., C.Bod., M.C., M.J., N.C-B., F.C-H., A.D., S.F., P.D., M.H., J.L-P., L.L., P.R., F.R., M.T., A.W-M., M.R., C.P., B.N.; Supervision, M.M., F.E.S., A.K., F.A., F.R-L.; Funding Acquisition, F.E.S., F.R-L.

All authors reviewed the manuscript.

Disclosure of Conflicts of Interest

L.D. is a former employee of Sanofi, France and may hold shares and/or stock options in the company. Other authors have nothing to disclose.

References

1. Kamnev A, Lacouture C, Fusaro M, Dupré L. Molecular Tuning of Actin Dynamics in Leukocyte Migration as Revealed by Immune-Related Actinopathies. Front Immunol 2021;12:750537.
2. Mastrogiovanni M, Juzans M, Alcover A, Di Bartolo V. Coordinating Cytoskeleton and Molecular Traffic in T Cell Migration, Activation, and Effector Functions. Front Cell Dev Biol 2020;8:591348.
3. Hodge RG, Ridley AJ. Regulating Rho GTPases and their regulators. Nat Rev Mol Cell Biol 2016;17(8):496–510.
4. El Masri R, Delon J. RHO GTPases: from new partners to complex immune syndromes. Nat Rev Immunol 2021;21(8):499–513.
5. Lougaris V, Baronio M, Gazzurelli L, Benvenuto A, Plebani A. RAC2 and primary human immune deficiencies. Journal of Leukocyte Biology 2020;108(2):687–96.
6. Su HC, Orange JS. The Growing Spectrum of Human Diseases Caused by InheritedCDC42 Mutations. J Clin Immunol 2020;40(4):551–3.
7. Chen Y, Chen Y, Yin W, et al. The regulation of DOCK family proteins on T and B cells. Journal of Leukocyte Biology 2021;109(2):383–94.
8. Dobbs K, Domínguez Conde C, Zhang S-Y, et al. Inherited DOCK2 Deficiency in Patients with Early-Onset Invasive Infections. N Engl J Med 2015;372(25):2409–22.
9. Engelhardt KR, Gertz EM, Keles S, et al. The extended clinical phenotype of 64 patients with DOCK8 deficiency. J Allergy Clin Immunol 2015;136(2):402–12.
10. Kunimura K, Uruno T, Fukui Y. DOCK family proteins: key players in immune surveillance mechanisms. International Immunology 2020;32(1):5–15.
11. Tunyasuvunakool K, Adler J, Wu Z, et al. Highly accurate protein structure prediction for the human proteome. Nature 2021;596(7873):590–6.
12. Linge P, Fortin PR, Lood C, Bengtsson AA, Boilard E. The non-haemostatic role of platelets in systemic lupus erythematosus. Nat Rev Rheumatol 2018;14(4):195–213.
13. Aslan JE, McCarty OJT. Rho GTPases in platelet function. J Thromb Haemost 2013;11(1):35–46.
14. Lin Q, Yang W, Baird D, Feng Q, Cerione RA. Identification of a DOCK180-related Guanine Nucleotide Exchange Factor That Is Capable of Mediating a Positive Feedback Activation of Cdc42*. Journal of Biological Chemistry 2006;281(46):35253–62.
15. Goggs R, Williams CM, Mellor H, Poole AW. Platelet Rho GTPases-a focus on novel players, roles and relationships. Biochem J 2015;466(3):431–42.

16. Gajardo T, Lô M, Bernard M, et al. Actin dynamics regulation by TTC7A/PI4KIIIα axis limits DNA damage and cell death during leukocyte migration [Internet]. Immunology; 2021 [cited 2022 Jul 19]. Available from: http://biorxiv.org/lookup/doi/10.1101/2021.10.14.464382
17. Mack NA, Georgiou M. The interdependence of the Rho GTPases and apicobasal cell polarity. Small GTPases 2014;5(2):10.
18. Park JH, Lee KH, Jeon B, et al. Immune dysregulation, polyendocrinopathy, enteropathy, X-linked (IPEX) syndrome: A systematic review. Autoimmun Rev 2020;19(6):102526.
19. Burchill MA, Yang J, Vogtenhuber C, Blazar BR, Farrar MA. IL-2 receptor beta-dependent STAT5 activation is required for the development of Foxp3+ regulatory T cells. J Immunol 2007;178(1):280–90.
20. Pleines I, Eckly A, Elvers M, et al. Multiple alterations of platelet functions dominated by increased secretion in mice lacking Cdc42 in platelets. Blood 2010;115(16):3364–73.
21. Pula G, Poole AW. Critical roles for the actin cytoskeleton and cdc42 in regulating platelet integrin alpha2beta1. Platelets 2008;19(3):199–210.
22. Nelson VS, Jolink A-TC, Amini SN, et al. Platelets in ITP: Victims in Charge of Their Own Fate? Cells 2021;10(11):3235.
23. Boilard E, Blanco P, Nigrovic PA. Platelets: active players in the pathogenesis of arthritis and SLE. Nat Rev Rheumatol 2012;8(9):534–42.
24. Dupré L, Boztug K, Pfajfer L. Actin Dynamics at the T Cell Synapse as Revealed by Immune-Related Actinopathies. Frontiers in Cell and Developmental Biology 2021;9:1046.
25. Gadea G, Blangy A. Dock-family exchange factors in cell migration and disease. European Journal of Cell Biology 2014;93(10–12):466–77.
26. Tangye SG, Pillay B, Randall KL, et al. Dedicator of cytokinesis 8-deficient CD4+ T cells are biased to a TH2 effector fate at the expense of TH1 and TH17 cells. J Allergy Clin Immunol 2017;139(3):933–49.
27. Moulding DA, Record J, Malinova D, Thrasher AJ. Actin cytoskeletal defects in immunodeficiency. Immunol Rev 2013;256(1):282–99.
28. Papa R, Penco F, Volpi S, Gattorno M. Actin Remodeling Defects Leading to Autoinflammation and Immune Dysregulation. Front Immunol 2021;11:604206.
29. Ridley AJ. Rho GTPase signalling in cell migration. Curr Opin Cell Biol 2015;36:103–12.
30. Sakabe I, Asai A, Iijima J, Maruyama M. Age-related guanine nucleotide exchange factor, mouse Zizimin2, induces filopodia in bone marrow-derived dendritic cells. Immun Ageing 2012;9:2.
31. Ma K, Du W, Wang X, et al. Multiple Functions of B Cells in the Pathogenesis of Systemic Lupus Erythematosus. Int J Mol Sci 2019;20(23):E6021.
32. Matsuda T, Yanase S, Takaoka A, Maruyama M. The immunosenescence-related gene Zizimin2 is associated with early bone marrow B cell development and marginal zone B cell formation. Immun Ageing 2015;12:1.
33. Tesch VK, Abolhassani H, Shadur B, et al. Long-term outcome of LRBA deficiency in 76 patients after various treatment modalities as evaluated by the immune deficiency and dysregulation activity (IDDA) score. J Allergy Clin Immunol 2020;145(5):1452–63.
34. Gámez-Díaz L, Neumann J, Jäger F, et al. Immunological phenotype of the murine Lrba knockout. Immunol Cell Biol 2017;95(9):789–802.
35. Wing JB, Tanaka A, Sakaguchi S. Human FOXP3+ Regulatory T Cell Heterogeneity and Function in Autoimmunity and Cancer. Immunity 2019;50(2):302–16.
36. Kim H-J, Barnitz RA, Kreslavsky T, et al. Stable inhibitory activity of regulatory T cells requires the transcription factor Helios. Science 2015;350(6258):334–9.

682 37. Chinen T, Kannan AK, Levine AG, et al. An essential role for the IL-2 receptor in
683 Treg cell function. Nat Immunol 2016;17(11):1322–33.
684 38. Kanai T, Jenks J, nadeau K. The STAT5b Pathway Defect and Autoimmunity.
685 Frontiers in Immunology [Internet] 2012 [cited 2023 Feb 24];3. Available from:
686 https://www.frontiersin.org/articles/10.3389/fimmu.2012.00234
687 39. Su HC. Insights into the pathogenesis of allergic disease from dedicator of cytokinesis
688 8 deficiency. Curr Opin Immunol 2023;80:102277.
689 40. Harada Y, Tanaka Y, Terasawa M, et al. DOCK8 is a Cdc42 activator critical for
690 interstitial dendritic cell migration during immune responses. Blood 2012;119(19):4451–61.
691 41. Keles S, Charbonnier LM, Kabaleeswaran V, et al. DOCK8 Regulates STAT3
692 Activation and Promotes Th17 Cell Differentiation. J Allergy Clin Immunol
693 2016;138(5):1384-1394.e2.
694 42. Janssen E, Morbach H, Ullas S, et al. Dedicator of cytokinesis 8-deficient patients
695 have a breakdown in peripheral B-cell tolerance and defective regulatory T cells. J Allergy
696 Clin Immunol 2014;134(6):1365–74.
697 43. Janssen E, Kumari S, Tohme M, et al. DOCK8 enforces immunological tolerance by
698 promoting IL-2 signaling and immune synapse formation in Tregs. JCI Insight 2(19):e94298.
699 44. Uhlen M, Oksvold P, Fagerberg L, et al. Towards a knowledge-based Human Protein
700 Atlas. Nat Biotechnol 2010;28(12):1248–50.
701 45. Ide M, Tabata N, Yonemura Y, et al. Guanine nucleotide exchange factor DOCK11-
702 binding peptide fused with a single chain antibody inhibits hepatitis B virus infection and
703 replication. Journal of Biological Chemistry [Internet] 2022 [cited 2023 Feb 18];298(7).
704 Available from: https://www.jbc.org/article/S0021-9258(22)00538-5/abstract
705

Table 1. Clinical and biological data of the cohort

Patients	**Patient A**	**Patient B**	**Patient C**	**Patient D1**	**Patient D2**	**Patient E**	**Patient F**	**Patient G**
AA change	p.L1298R	p.H1336R	p.T275S	p.D414Y	p.D414Y	p.L1706S	p.R1366Q	p.R1885C
Age (year)	14	7	29	20	20	20	6.5	14
Clinical manifestations								
Age at onset (year)	1.4	5	5	14	9	3	5	5
Autoimmune manifestations	Severe ITP	RF Polyarticular JIA	Evans	SLE	SLE	Evans	AI neutropenia	Evans
Skin manifestation	Sweet syndrome, panniculitis	-	Folliculitis	Oral discoid LE	Bullous cutaneous SLE	-	Ecthyma gangrenosum	-
Digestive manifestation	Severe IBD (ileo-colitis)	Colon Cryptitis	-	Ileitis	-	-	Anal and oral ulcers Intermittent diarrhea	-
Others	Non regenerative anemia	Hemolytic anemia	-	PID, Growth retardation	Growth retardation	-	Auto-inflammatory syndrome, Lymphoproliferation, underweight	-
Therapies	Corticosteroids, IVIG, rituximab, azathioprine, everolimus, infliximab	Corticosteroids, methotrexate, adalimumab	Corticosteroids	Corticosteroid, MMF, HCQ, belimumab	Steroids, HCQ	IVIG, corticosteroids	Antibiotics	Corticosteroids, Rituximab, sirolimus
Immunophenotypage	Defect memory and transitional B cells	Normal B cells, T and NK lymphopenia, NC	Excess of $CD21_{low}$ B cells, B cell lymphopenia, diminished MZB and switched memory B cells	Excess $CD21_{low}$ and transitional B cells, diminished MZB	Excess $CD21_{low}$ and transitional B cells, NK lymphopenia	Normal, NC	Global lymphopenia, excess of $CD21_{low}$ and transitional B cells	Diminished switch memory B cells and excess of transitional B cells
Immunoglobulin dosage	Value / Reference values	Value / Reference values	Value / Reference values	Value	Value / Reference values	Value / Reference values	Value / Reference values	Value / Reference values
gr/L	IgG 14 6.6-15.3 IgA 2.15 0.5-2.2 IgM 0.25 0.53-1.62	IgG N - IgA N IgM N	IgG 1.24 6.6-15.3 IgA <0.05 0.5-2.2 IgM 0.46 0.53-1.62	γ 26.3 g/L	γ 17 gr/L 6.9-15	IgG 10.73 6.44-11.96 IgA 1.24 0.63-2.02 IgM 0.42 0.416-1.31	IgG 27 5.5-11.15 IgA 3 0.4-1.6 IgM 7 0.5-1.5	IgG 3.69 6.6-15.3 IgA 0.16 0.5-2.2 IgM 0.25 0.53-1.62
Autoantibodies	ANCA, anti-αIIbβ3, ANA, anti-TPO, anti-thyroglulin	RF, +IgG Coombs	+ IgG Coombs	ANA, RF,anti-RNP, anti-Sm	ANA, RF,anti-RNP, anti-Sm	+IgG Coombs	weak + anti-CD16	+ IgG and complement Coombs

Table 1 – Clinical and biological phenotypes of *DOCK11* mutated patients

Listed are reference ranges or laboratory values for the patients' age groups. Therapy refers to all therapies that patients received.

ITP: immune thrombocytopenia, IBD: inflammatory bowel disease, JIA: Juvenile Idiopathic Arthritis, SLE: Systemic Lupus erythematosus, AI neutropenia: Autoimmune neutropenia, LE: Lupus erythematosus, PID: pulmonary interstitial disease. IVIG: intravenous immunoglobulins, MMF: mycophenolate mofetil, HCQ: hydroxychloroquine. NC: denotes for Not complete B phenotype, MZB: marginal zone B cells ,N: normal values, γ: gamma-globulins detected in serum protein electrophoresis, ANCA: anti-neutrophil cytoplasmic antibody , ANA: antinuclear antibodies, Anti-αIIbβ3: antibody against Integrin alpha-IIb/beta-3, TPO: Thyroid Peroxidase antibody, RF: Rheumatoid Factor, Anti-RNP: Anti-Ribonucleoprotein antibody, Anti-Sm: Anti-smooth muscle antibody , + IgG Coombs: positive direct Coombs with detection of IgG, + IgG and complement Coombs: positive direct Coombs with detection of IgG and C3.

Figure 1 - *DOCK11* hemizygous mutations: structural consequences and protein expression: Panel **(A)** shows dermatological clinical findings of DOCK11 deficiency patients (from left to right): lobular panniculitis on feet in Patient A, bullous cutaneous SLE in Patient D2, non-infectious ecthyma gangrenosum on external lateral border of the right foot in Patient F. **(B)** Schematic overview of DOCK11 protein with the positions of patients' DOCK11 mutations. Molecular partners described to interact with DOCK11 are mentioned below the domain they bind. **(C)** 3D structure of human DOCK11, as predicted by AlphaFold2 (ribbon representation, except for DRH2 which is shown as a blue surface). Confidence is high (pLDDT>90) for the individual domain 3D structures, whereas the 3D structure of the N- and C-terminal sequences, linkers between domains and large loops (often disordered) remain elusive (low pLDDT values - asterisks). Two such very large loops are depicted with broken lines, with the amino acid intervals. Positions of the domains relative to each other also remain uncertain, except form the C2-DHR1 interface (very low PEA (predicted error alignment) values). Mutated amino acids are depicted in magenta (Patients A, B, C, D and F). D414 is predicted exposed at the surface of the C2 domain and likely to play a significant role in the C2-DRH1 interface (Fig. S6A-C). L1298 is predicted with confidence as being buried with the hydrophobic core of the ARM repeats, conserved in DOCK-C proteins (Fig. S6D). The region including H1336 and R1366, more variable and predicted with a lower confidence, is located at the concave surface of the ARM repeats, where interactions take place in complexes of other DOCK proteins with partners. **(D)** 3D structure of DHR-2 domain of human DOCK11, as predicted by AlphaFold2. The DHR-2 (in light blue) is represented interacting with CDC42 (in gray), as deduced from the superimposition of DOCK11 with the 3D structure of DOCK9 in complex with CDC42. Mutated amino acids are depicted in magenta and correspond to patients E and G mutations. L1706 is in the hydrophobic core of DHR2 lobe A, important for dimerization. R1885 is part of DHR2 lobe B, which consists of two sheets predicted in direct contact with the switch 1 domain of CDC42. **(E)** DOCK11 expression was evaluated in activated T cells of healthy donors (HDs) and patients (A, B, C, D1, F and G) by Western blotting. Dotted lines indicate that the samples were derived from the same gel but were non-contiguous. The graph shows the relative expression of DOCK11 versus HDs (set to 1) ± SEM after normalization against Ku-70 expression).

Figure 2 - Study of platelets from *DOCK11* mutated patients: (A) DOCK11 expression was evaluated in platelets of healthy donors (HDs) and patients (A, C, D1, D2, F and G) by Western blotting. Dotted lines indicate that the samples were derived from the same gel but were non-contiguous. The graph shows the mean of the relative expression of DOCK11 versus HD (set to 1) ± SEM after normalization against β-actin expression from several independent experiments (HDs, n = 69; A, n = 22; C, n = 14; G, n = 16; D1, D2, n = 8; F, n = 15). Statistical difference was evaluated by one-way ANOVA with Dunnett's correction test for multiple comparisons (*$p < 0.05$; ***$p < 0.001$). **(B)** Platelet count for each patient (A, C, D1, D2, F, G) was determined by automated blood cell counter. Shaded area represents the normal range between 150 x 10^9 and 400 x 10^9 platelets/L. Patients A and C were investigated for their platelet count several times (2 and 3 times, respectively). **(C)** Platelet size was evaluated by flow cytometry. Each dot represents the mean size measured by the mean forward scatter height (FSC-H; a.u., arbitrary units) of washed platelets from healthy donors (HDs) and patients. The box-and-whisker plot shows the normal range, determined from HDs. Whiskers represent the 5-95 percentiles, the box correspond to the interquartile range, the center line is the median and the cross indicates the mean of 65 platelets. **(D)** Platelet ultrastructure which was analyzed once for each patient using transmission electron microscopy (TEM). Scale bar represents 1 µm. **(E, F)** TEM analysis of platelet ultrastructure in each patient. Platelet surface (E) and platelet shape (F) which is defined as the ratio between the largest diameter and the smallest diameter are derived from the TEM images. Graphs represent the mean ± SEM of at least 1100 HD's platelets and 100 patient's platelets. Statistical significance was determined in a one-way ANOVA with the Dunnett's post-test for multiple comparisons. **(G)** Graph represents the mean percentage ± SEM of discoid platelets (dark grey), platelet with filopodia (light grey) and platelets with lamellipodia or full spreading (white) of at least 150 analyzed platelets from several independent experiments (HDs, n=17; patient A, n=4; patient C, n=3). Statistical significance was determined only for patients A and C compared to HDs in a one-way ANOVA with the Dunnett's post-test for multiple comparisons (* $p < 0.05$; ** $p < 0.01$). Patients D1, D2, F and G were not statistically analyzed since only one experiment was performed. Scale bar represents 10 µm. **(H)** Spreading of HD and patients' platelets onto fibrinogen matrix for 30 minutes was analyzed by epifluorescence microscopy in the presence of apyrase (5 U/mL) and indomethacin (4.5 µM). Platelet morphology was visualized using F-actin detection by fluorescently labeled-phalloidin. **(I)** CDC42 activity evaluated in HDs' platelets and patients' platelets by G-LISA after stimulation by 0.5 U/mL thrombin for 1 minute in unstirred conditions. Graph represents the relative CDC42 activity of each patient compared to that of HD (set to 100%).

Figure 3 - *DOCK11* mutations lead to abnormal cell morphologies: Spreading assays with different lymphocytes subsets. **(A)** T cell morphologies after spreading. Blue color corresponds to DAPI staining (nucleus). Red color corresponds to actin staining. Each patient is represented by a different symbol: Patient A (⁕), patient B (●), patient C (■), patient D1 (×), patient D2 (★), patient F (▽), patient G (**o**). Coverslips were coated with either poly-L-lysine (i); poly-L-lysine, anti-CD28 and anti-CD3 (0,1µg/mL) antibodies (ii); or poly-L-lysine, anti-CD28 and anti-CD3 (1µg/mL) antibodies (iii). Scale is set at 10µm. Cell area was measured with or without CN02 treatment (CDC42/RAC1 activator). Non-parametric Kruskal-Wallis' test was performed (*$p < 0.05$). **(B)** B-lymphoblastic cell lines morphologies after spreading. Several morphologies were observed: cells with no protrusion, cells spread along one axis, cells with fine protrusions (filopodia), cells with lamellipodia and cells presenting both lamellipodia and filopodia. Cells patients presented abnormal protrusions. Repartition of each morphology types is shown. Scale is set at 10µm. **(C)** Morphologies of mature monocyte-derived dendritic cells (MDDC) from healthy donor, either using a scramble sh-RNA or a *DOCK11*-sh-RNA, after stimulation with LPS 100ng/ml (Lipopolysaccharide) for 24 hours, were observed using scanning electron microscopy (SEM). Scale is set at 5 µm.

Figure 4 - DOCK11 is needed for human leukocytes migration under confinement: Analysis of human healthy donor (HD) and DOCK11-deficient T cell migration in fibronectin-coated microchannels. Boxes include the 80% of the points and bars represent the higher and lower 10% of points. **(A)** Representative montage of the change of position over time of human T cell blast migrating inside microchannels of 4x 5µm with a timelapse of 2 min. **(B)** Representative kymograph of T cell blast from Healthy Donors (HD, top panel) and DOCK11 patients (A – E, lower panels as indicated). **(C)** Mean instantaneous speed of HD and DOCK11 T cell blasts migrating in 4 x 5µm microchannels. Results from n=2 independent experiments with each condition. Unpaired non-parametric Mann-Whitney test was used to evaluate statistical significance between the mean speeds of controls and patients (* $p < 0.05$; ** $p < 0.01$; *** $p < 0.001$). **(D)** Density maps representing the enrichment of actin in HD and DOCK11 deficient T cells migrating in 8 x 5 µm microchannels. Cells were allowed to migrate and fixed with 4% PFA to maintain the polarized morphology and stained with phalloidin to visualize F-actin. The density maps were generated by averaging the signal from HD n= 85, DOCK11A n=32, DOCK11D n=46 and DOCK11E n=63 cells. Quantification of the signal intensity on density maps presented as front/rear ratio per cell. One-way ANOVA was used to evaluate statistical significance. **(E)** Mean instantaneous speed of HD and DOCK11 T cell blasts (patient G) migrating in 4 x 5µm microchannels, with or without RAC inhibitor treatment. Results from n=2 independent experiment with each condition. One-way ANOVA test was used to evaluate statistical significance. Unpaired non-parametric Mann-Whitney test was used to evaluate statistical significance between the mean speeds of controls and treated controls, patient and treated patient (* $p < 0.05$).

Figure 5. Immune phenotype by mass cytometry

(A) UMAP (Unifolm Manifold Approximation and Projection) of immune cell subsets clusters analyzed by mass cytometry on whole blood samples from DOCK11 patients (n= 7) and age-matched healthy donors (n=6). Each cluster is color coded. **(B)** Cell cluster biases observed between DOCK11 patients and healthy donors. DOCK11 patients have a significantly lower percentage of $CD56_{bright}$ NK, late NK cells, MAIT, and memory B cells. Two-tailed p-values were determined with a nonparametric Mann-Whitney test. (*) p-value < 0.05; (**) p-value < 0.01; (***) p-value < 0.005.

Figure 6. Treg phenotype and STAT5 activation

(A) FoxP3 mean fluorescence intensity on Tregs from Healthy donors (HDs) and DOCK11 patients. Treg are defined by CD4+ CD25+ CD127low as depicted in the graph on the right side of the panel. **(B)** Representative dotplots of CD3+ CD4+ Foxp3+ Helios+ cells from healthy donors (HDs) and two DOCK11 patients. **(C)** Representative histograms of phospho-STAT5 in T, CD25+ T and B cells from healthy donors and DOCK11 patients. Cells were stimulated for 60 min with IL2. Results for unstimulated (NS) cells are shown with the black peak. **(D)** Kinetics of phospho-STAT5 expression upon IL2 stimulation: unstimulated (NS), 15 and 60 minutes. Mean fluorescence intensity (MFI) of phospho-STAT5 in T, CD25+ T, MAIT and B cells from healthy donors (HDs) and DOCK11 patients.

Figure 1: DOCK11 mutations

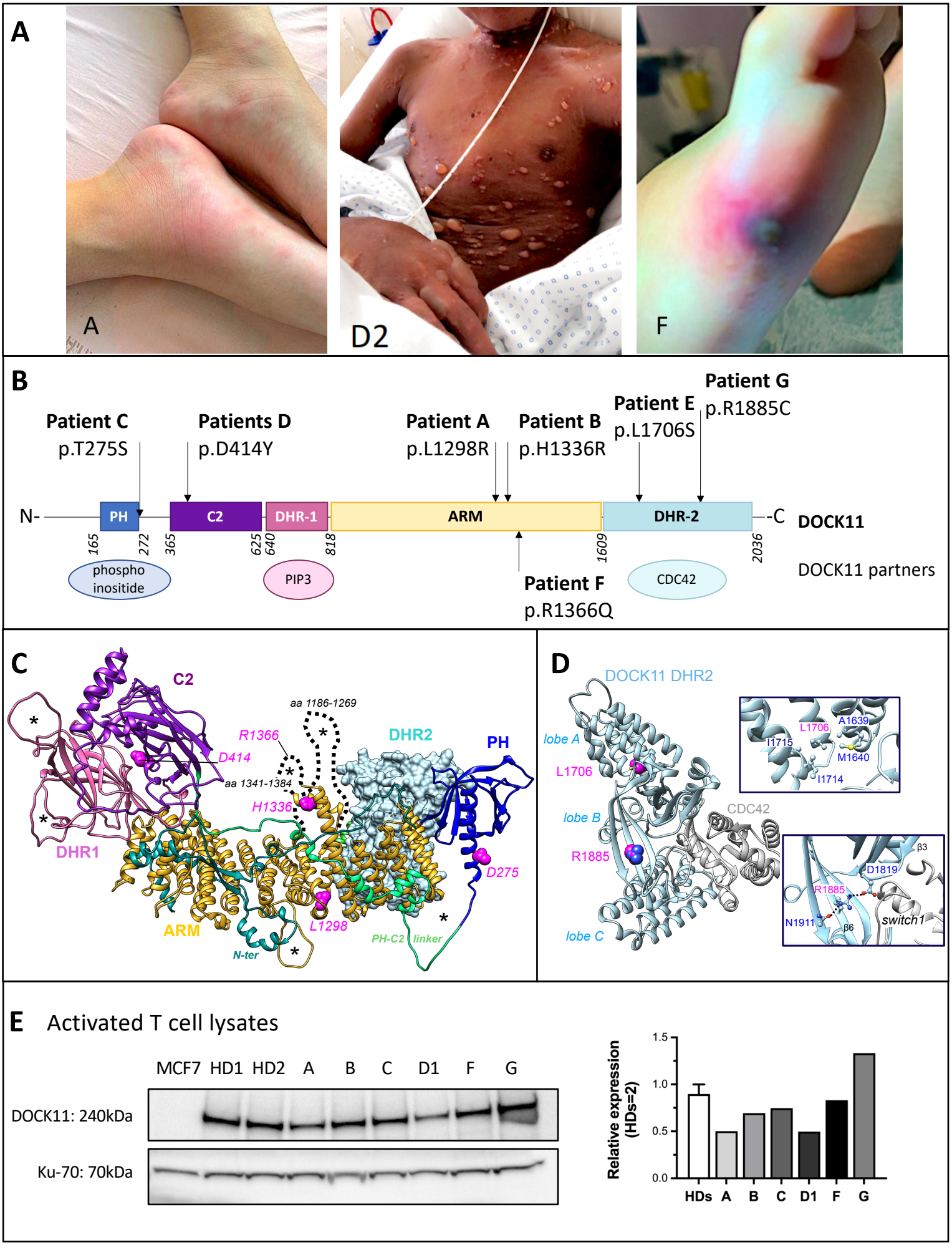

Figure 2: Platelets' study

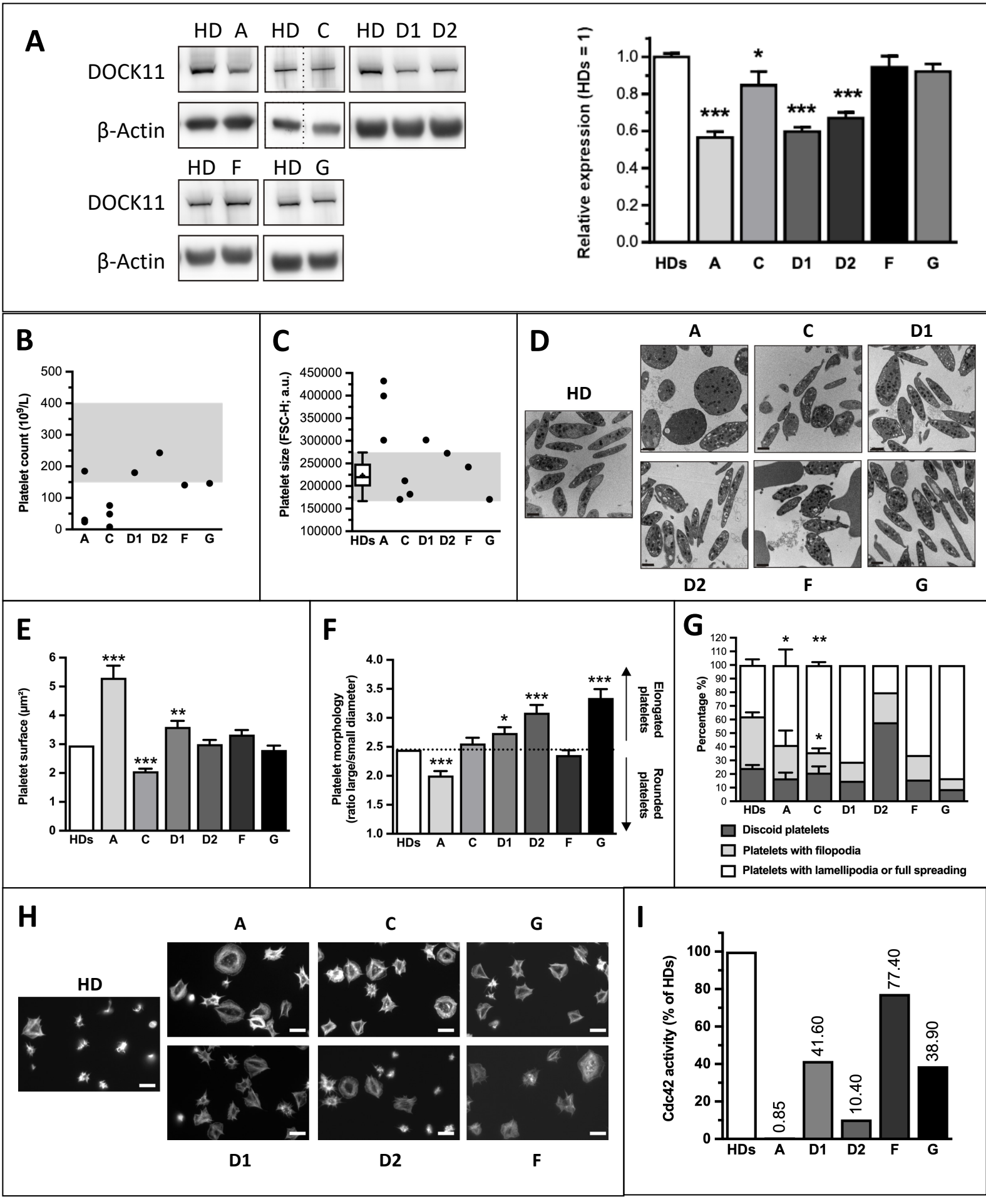

Figure 3: Morphological impairment after spreading

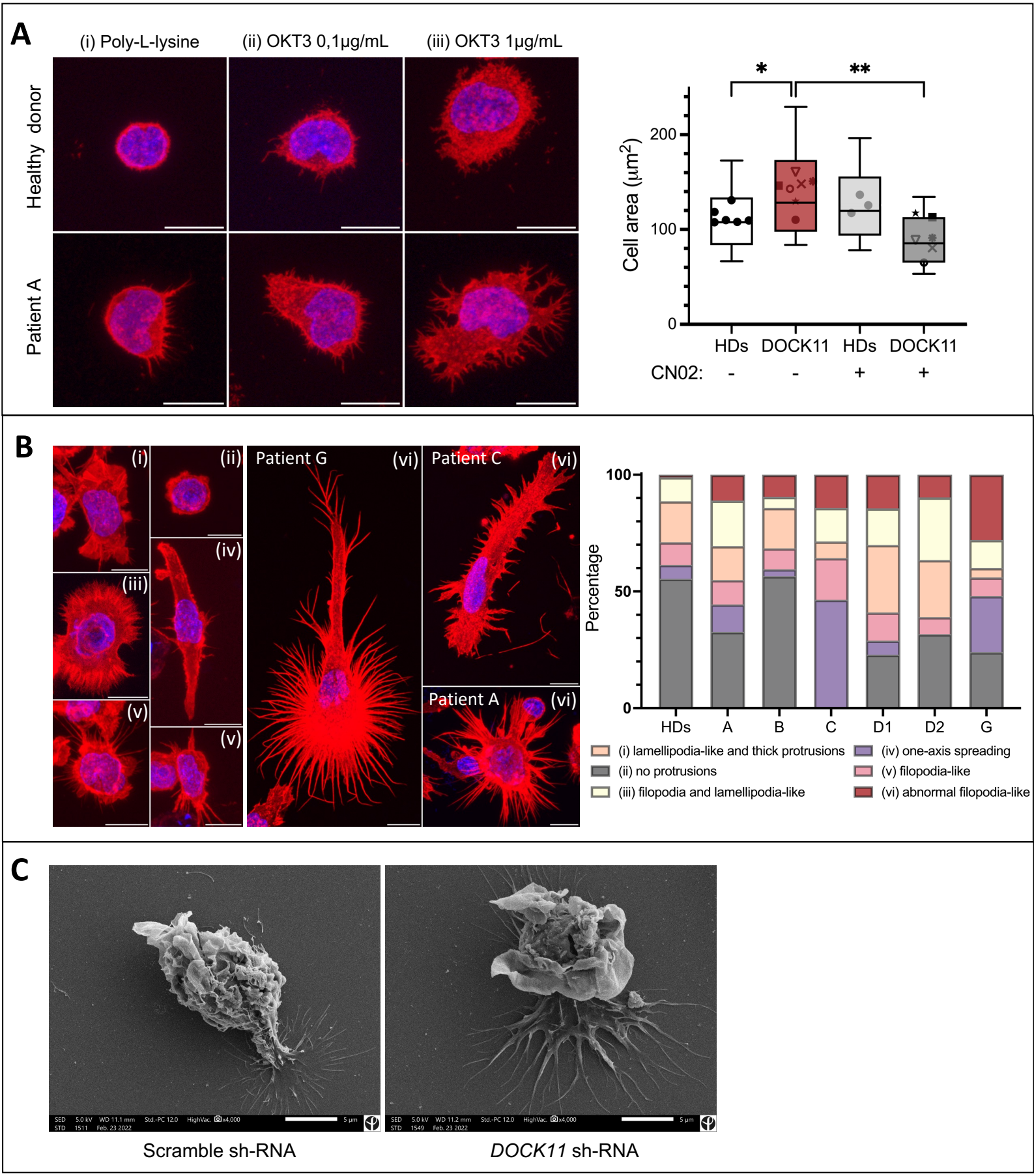

Figure 4: Migration assays – reflecting reduced CDC42 activity

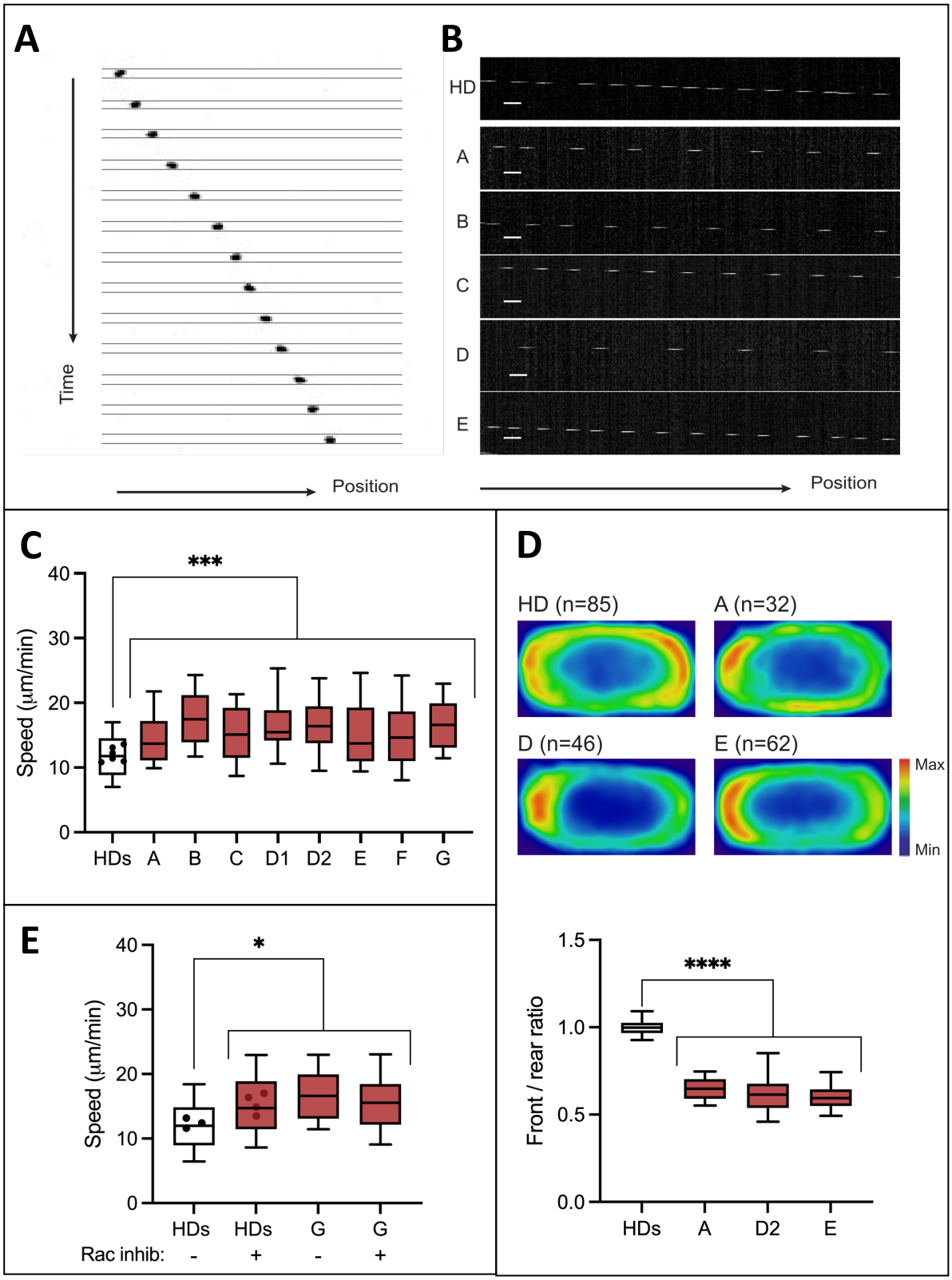

Figure 5: Immune phenotype by CyTOF

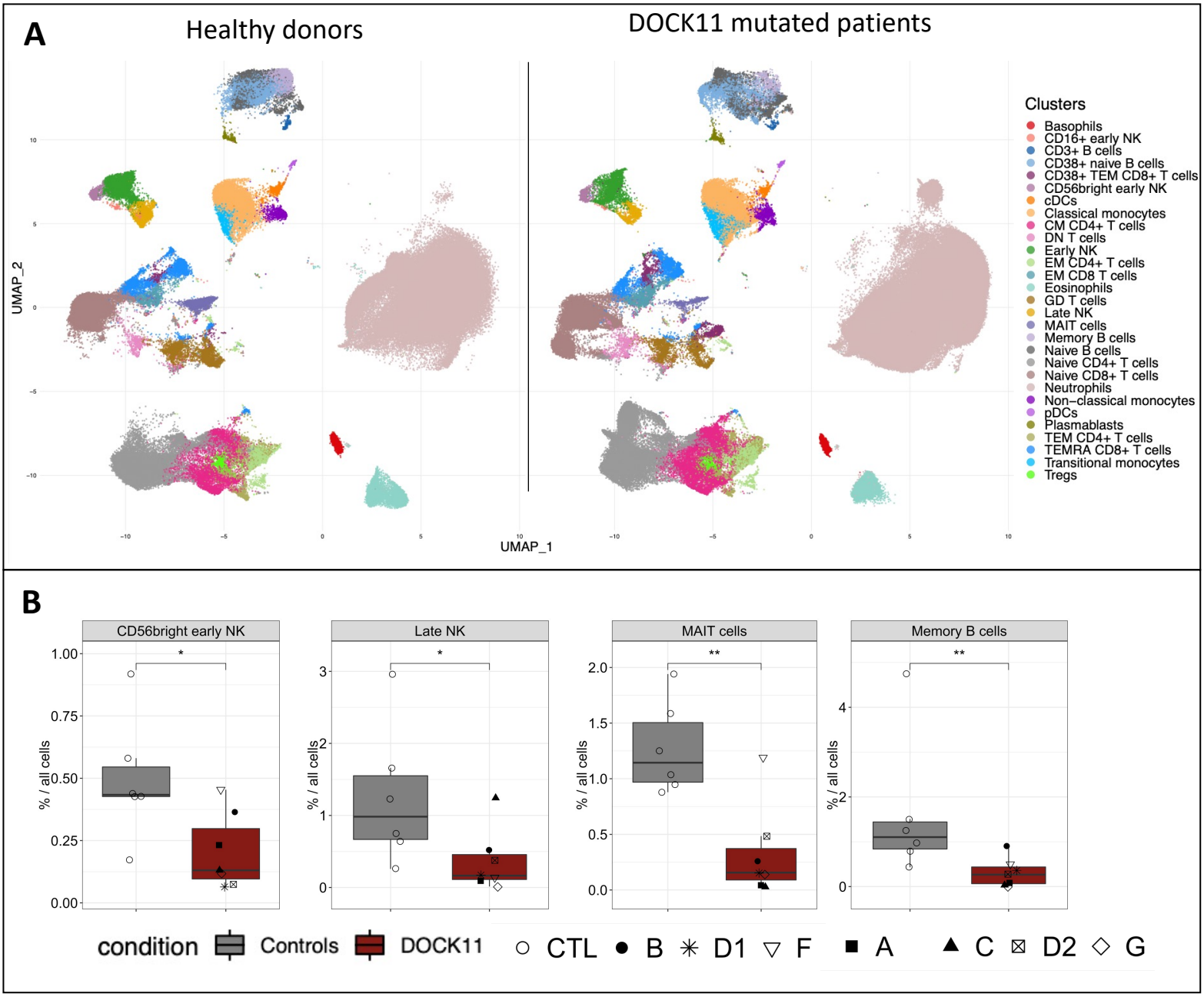

Figure 6: Treg phenotype and STAT5 activation